

## STRUCTURE DETERMINATION OF ALTEMICIDIN BY NMR SPECTROSCOPIC ANALYSIS

Atsushi Takahashi, Hiroshi Naganawa, Daishiro Ikeda\* and Yoshiro Okami

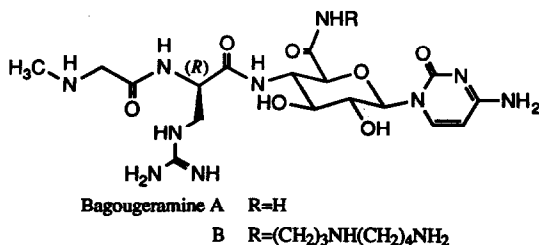
Institute of Microbial Chemistry  
 3-14-23 Kamiosaki, Shinagawa-ku, Tokyo, 141 Japan

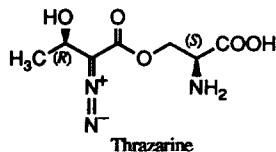
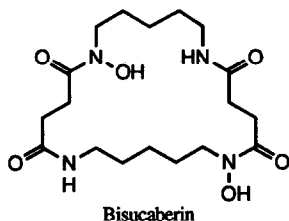
(Received in USA 27 November 1990)

**SUMMARY:** Recently various pulse experiments using the high field NMR spectrometer are available to study structures of only truly small amounts of natural products. In the course of our research on the screening of new antibiotics, we isolated altemicidin which showed anti-brine shrimp activity. The relative structure of altemicidin was determined by NMR spectroscopic analysis which included  $^1\text{H}$ ,  $^{13}\text{C}$ ,  $^1\text{H}$ - $^1\text{H}$  COSY, HMQC and HMBC spectra.

Antibiotics research has provided many attractive problems for the scientist, e.g. screening programs, isolation techniques and structure determinations. The isolation and structure determination of antibiotics which are available in only small quantities are important tasks facing organic chemists. Fortunately, modern techniques for structural studies require only minimal quantities of antibiotics. X-ray crystallographic analysis is the most favorable method if a suitable crystal can be obtained; otherwise NMR and mass spectroscopic studies are very powerful techniques. Nowadays, high magnetic field instruments and various pulse experiments in NMR spectrometry and soft ionization methods in mass spectrometry are applicable to study structures of antibiotics.

Recently, we isolated new antibiotics bagougeramines,<sup>1,2)</sup> bisucaberin,<sup>3,4)</sup> thrazarine<sup>5,6)</sup> and

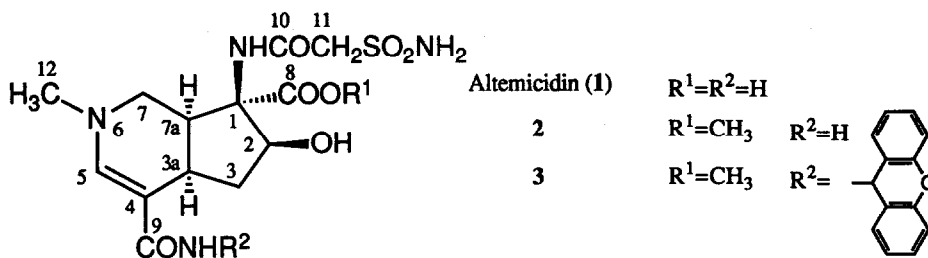




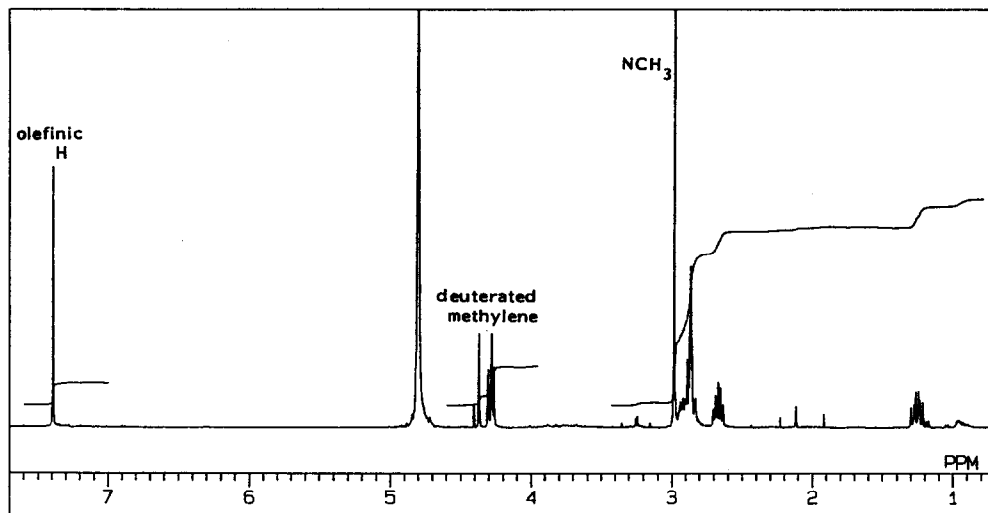
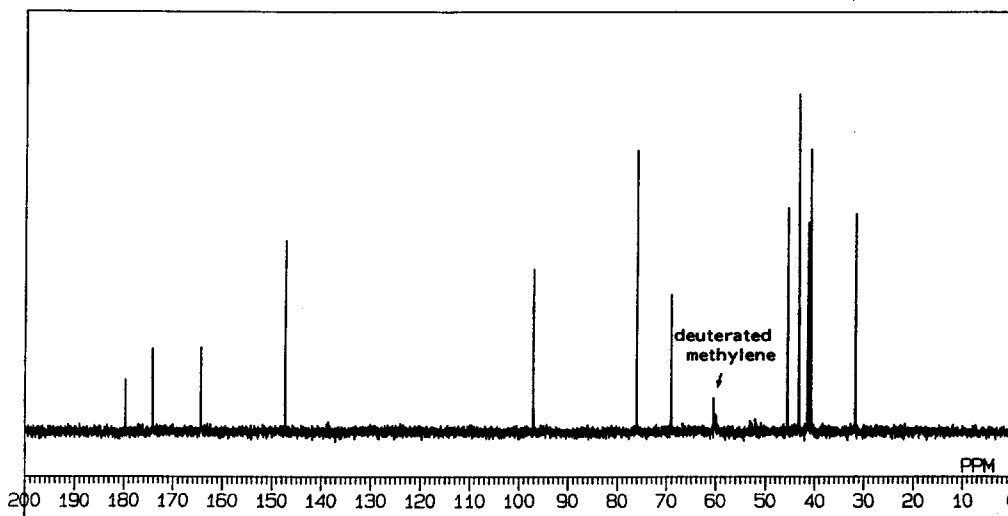
altemicidin<sup>7,8</sup>) by a variety of screening systems, *i.e.* the pattern of aminoglycoside antibiotic resistance, enhancement of macrophage-mediated lysis of tumor cells and anti-brine shrimp activity. Structure elucidations were carried out mainly using classical degradation experiments for bagougeramines, X-ray crystallography for bisucaberin and thrazarine and NMR spectroscopic analysis for altemicidin. In this report, we disclose NMR spectroscopic studies on altemicidin in detail.

## RESULTS AND DISCUSSION

The screening of new insecticidal and acaricidal antibiotics was carried out with reference to anti-brine shrimp activity from actinomycete strains isolated from the marine environment. One isolate identified as *Streptomyces siyoaensis* SA-1758 was found to produce a substance having anti-brine shrimp activity as well as acaricide and antitumor activity.<sup>7)</sup>



Altemicidin (1) was purified by activated charcoal, Diaion<sup>®</sup> CHP-20 and Sephadex<sup>®</sup> LH-20 column chromatographies, successively, from cultured broth of *S. siyoaensis* SA-1758. The molecular formula of 1 was established as  $C_{13}H_{20}N_4O_7S$  by elemental analysis and mass spectrometry. SIMS showed the molecular ion at  $m/z$  377 [(M+H)<sup>+</sup>] and negative HRFABMS at  $m/z$  375.1009 [(M-H)<sup>-</sup>, calcd for  $C_{13}H_{19}N_4O_7S$ : 375.0975]. The IR spectrum of 1 indicated the presence of an amide group (1650 and 1550  $cm^{-1}$ ) and sulfonyl

Fig. 1.  $^1\text{H}$  NMR spectrum of 1 in  $\text{D}_2\text{O}$ .Fig. 2.  $^{13}\text{C}$  NMR spectrum of 1 in  $\text{D}_2\text{O}$ .

group (1345 and 1165  $\text{cm}^{-1}$ ). As initial attempts to grow crystals of **1** suitable for X-ray crystallographic analysis failed, we used the new NMR techniques for determining the structure.

First, normal  $^1\text{H}$  and  $^{13}\text{C}$  NMR spectra of **1** in  $\text{D}_2\text{O}$  were recorded. As shown in Fig. 1, an olefinic proton at  $\delta$  7.39 and *N*-methyl protons at  $\delta$  2.98 were observed and at  $\delta$  4.32 isolated methylene protons (AB quartet) having reduced intensity were also observed. Fig. 2 shows thirteen carbon signals including a multiplet at  $\delta$  60.3 which corresponds to the isolated methylene group. The splitting of this carbon signal was due to substitution by deuteriums in  $\text{D}_2\text{O}$ . Since it turned out that **1** contained an easily exchangeable function with deuteriums in  $\text{D}_2\text{O}$  other than OH and NH groups, subsequent NMR spectroscopic studies were carried out in an aprotic solvent. Unfortunately, the  $^1\text{H}$  NMR spectrum of **1** in DMSO- $d_6$  contained broadened signals.

Table 1. The conditions of the 1D NMR spectra of **1**.

	$^1\text{H}$ NMR	$^{13}\text{C}$ NMR	DEPT-135°
Observing Nucleus	$^1\text{H}$	$^{13}\text{C}$	$^{13}\text{C}$
Observing Frequency (MHz)	400	100	100
RF Carrier Position (ppm)	4.9	100	100
Data Point	32,768	32,768	32,768
Spectral Width (Hz)	5,000.0	23,041.5	23,041.5
Acquisition Time (s)	3.277	0.711	0.711
Delay Time (s)	2.0	1.3	1.0
Scan Times	16	2,216	680
Pulse Width $^{13}\text{C}$ ( $\mu\text{s}$ )	-	5.0 (45°)	10.0 (90°)
$^1\text{H}$ ( $\mu\text{s}$ )	7.0 (45°)	-	39.0 (135°)
$^1\text{H}$ ( $\mu\text{s}$ )	-	-	26.0 (90°)
$\Delta$ , 1/2 $J_{\text{CH}}$ (ms)	-	-	3.70
$^1\text{H}$ Irr. Carrier Position (ppm)	-	4.8	4.8
$^1\text{H}$ Irr. RF Power (watt)	-	~4	~4

Next, the spectroscopic analysis was performed by using a methyl ester derivative of **1** in an aprotic solvent. Treatment of **1** with trimethylsilyldiazomethane gave methyl ester (**2**), SIMS  $m/z$  391 [(M+H) $^+$ ].  $^1\text{H}$  and  $^{13}\text{C}$  NMR spectra of **2** in pyridine- $d_5$  are shown in Figs. 3 and 4. All protons and carbons of **2** were clearly observed in each spectrum. A distortionless enhancement by polarization transfer<sup>9</sup> (DEPT) experiment provided the multiplicity of carbon signals. Correlations between protons were obtained by  $^1\text{H}$ - $^1\text{H}$  shift correlation spectroscopy<sup>10</sup> ( $^1\text{H}$ - $^1\text{H}$  COSY) and one-bond shift correlations between proton and carbon were given by  $^1\text{H}$ -detected heteronuclear multiple-quantum coherence<sup>11,12</sup> (HMQC) experiments. Employment of HMQC experiments which use observation of the  $^1\text{H}$  rather than the  $^{13}\text{C}$  nucleus greatly enhances the sensitivity of the  $^1\text{H}$ - $^{13}\text{C}$  shift correlation and makes it possible to use much smaller amounts of the sample and to save time. The

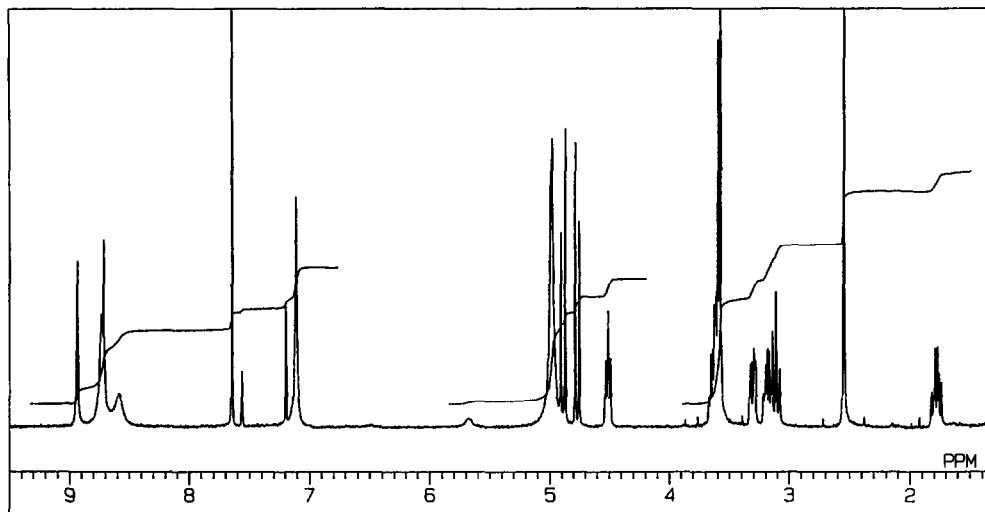
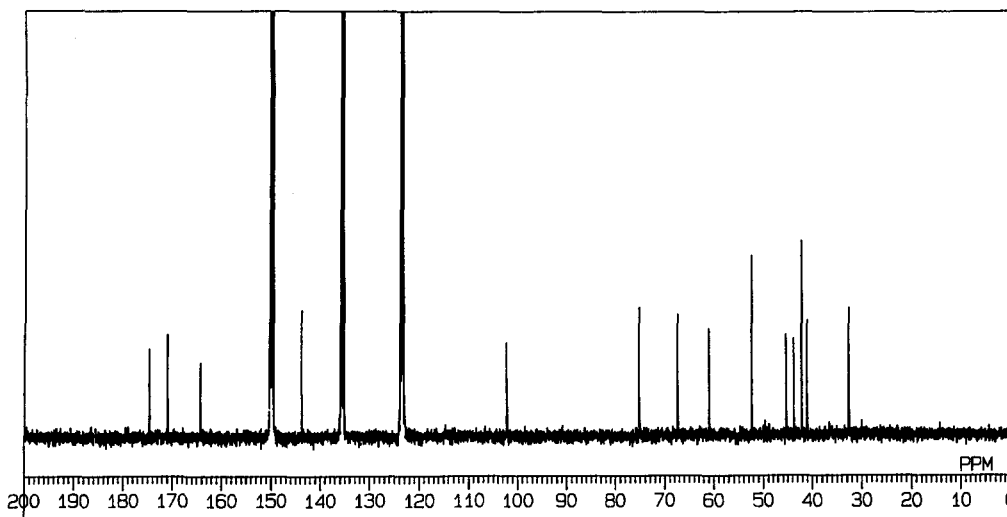
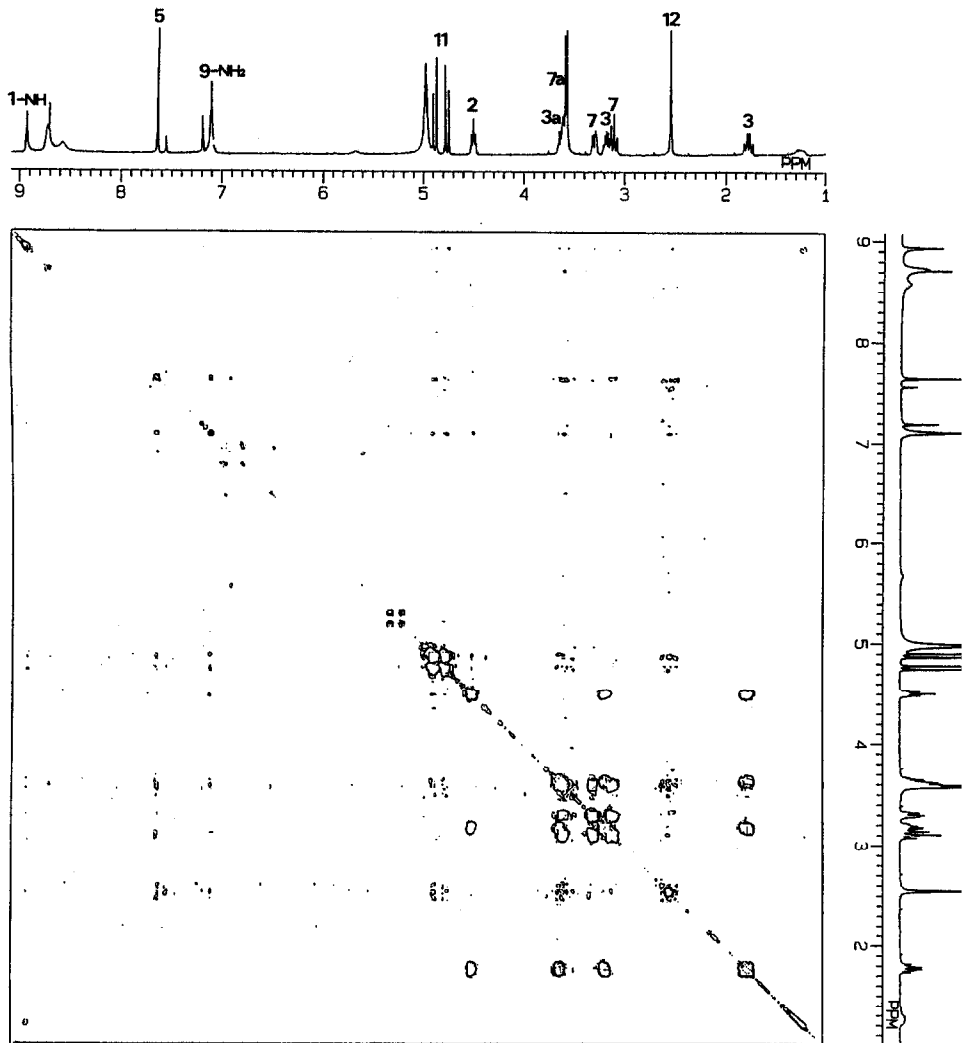
Fig. 3.  $^1\text{H}$  NMR spectrum of **2** in pyridine- $d_5$ .Fig. 4.  $^{13}\text{C}$  NMR spectrum of **2** in pyridine- $d_5$ .

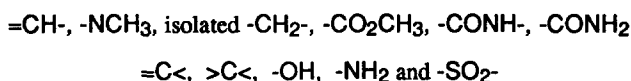
Fig. 5.  $^1\text{H}$ - $^1\text{H}$  DQF COSY of 2.

conditions of measurements of these experiments (1D and 2D NMR spectra) are listed in Tables 1 and 2. The  $^1\text{H}$ - $^1\text{H}$  COSY spectrum is shown in Fig. 5. A proton at  $\delta$  1.77 was coupled to protons at  $\delta$  3.19, 3.64 and 4.50,

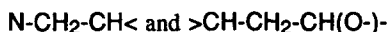
Table 2. The conditions of the 2D NMR spectra of 2.

		HMBC	HMQC	DQF COSY
Observing Nucleus		$^1\text{H}$	$^1\text{H}$	$^1\text{H}$
Observing Frequency	(MHz)	400	400	400
RF Carrier Position	(ppm)	4.9	4.9	4.9
Data Point in $F_2$		1024	1024	1024
Spectral Width in $F_2$	(Hz)	3,230.0	3,230.0	3,230.0
Data Point in $F_1$		256	256	256
Spectral Width in $F_1$	(Hz)	20,000	20,000	3,230.0
Acquisition Time	(s)	0.159	0.159	0.159
Delay Time	(s)	1.0	1.0	1.0
Scan Times per $t_1$ value		176	176	16
Pulse Width $^1\text{H}$ 90°	( $\mu\text{s}$ )	14	14	14
$^{13}\text{C}$ 90°	( $\mu\text{s}$ )	10	10	-
$\Delta_1$	(ms)	3.704	3.704	-
$\Delta_2$	(ms)	60	-	-
Total Measuring Time	(h)	14.5	15	1.5

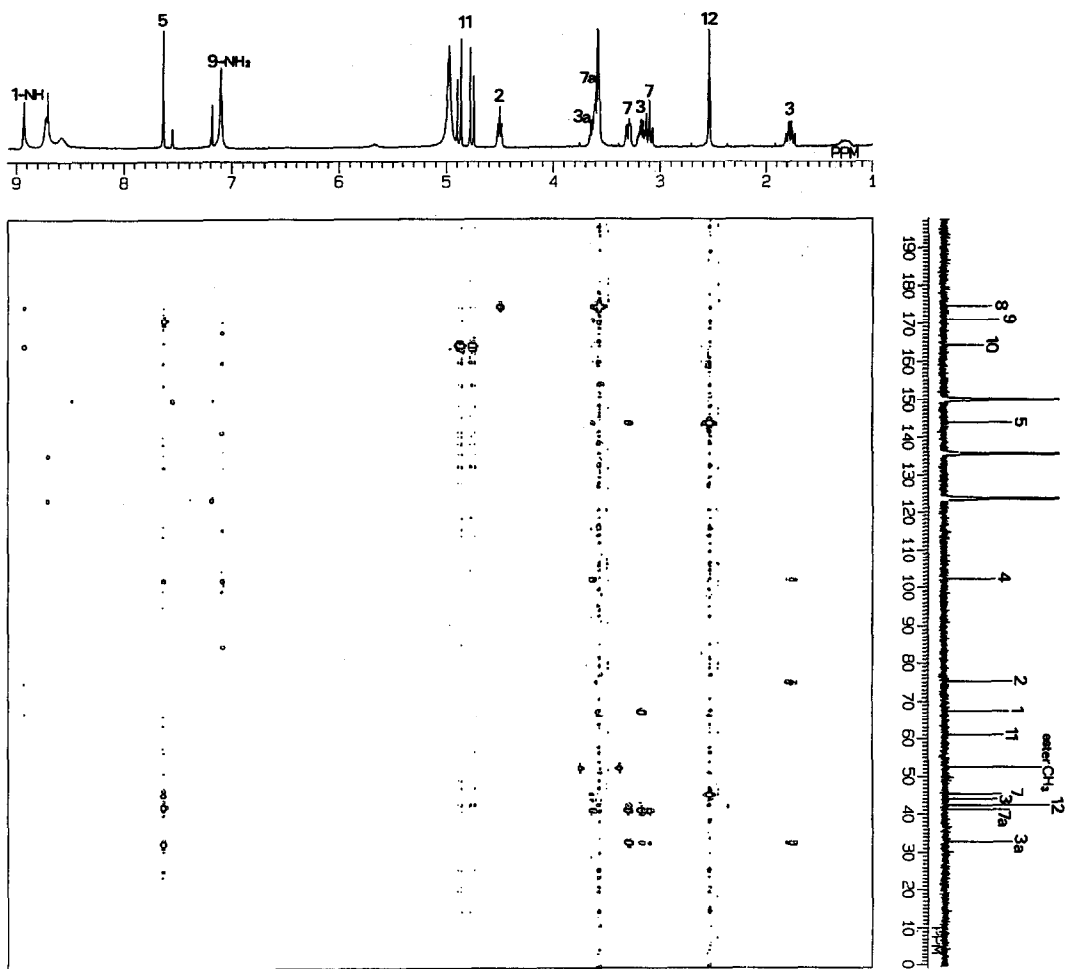
and a proton at  $\delta$  3.19 was coupled to protons at  $\delta$  1.77, 3.64 and 4.50. This suggested that these two protons ( $\delta$  1.77 and 3.19) are attached to the same carbon in a methylene group. This observation was confirmed by the HMQC experiment. Cross peaks between a carbon at  $\delta$  43.8 and protons at  $\delta$  1.77 and 3.19 were shown. Results of NMR experiments and other physico-chemical properties revealed the following fragments in the structure of 2:



Additionally, the presence of two carbon chains were indicated:

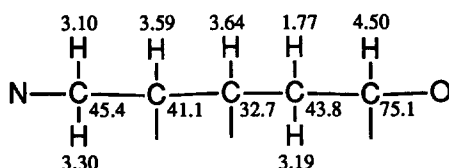


None of the experiments described above presents unambiguous information about the further carbon sequence. This problem was solved using the recently developed  $^1\text{H}$ -detected heteronuclear multiple-bond correlation<sup>12)</sup> (HMBC) technique. The conditions of the HMBC spectral measurements are listed in Table 2 and the spectrum is shown in Fig. 6. The olefinic proton (5-H,  $\delta$  7.64) attached directly to C-5 ( $\delta$  143.7) showed

Fig. 6. HMBC spectrum of **2**.



connectivities to a non-protonated olefinic carbon (C-4,  $\delta$  102.2), a bridge-head carbon (C-3a,  $\delta$  32.7), a methylene carbon (C-7,  $\delta$  45.4), a primary amide carbonyl carbon (C-9,  $\delta$  171.0) and *N*-methyl carbon (C-12,  $\delta$  42.2). Although no cross peak was observed between methine protons at 3a ( $\delta$  3.64) and 7a ( $\delta$  3.59) in the  $^1\text{H}$ - $^1\text{H}$  COSY spectrum, the HMBC spectrum showed connectivity between 3a-H and a methine carbon (C-7a,  $\delta$  41.1). Furthermore, methylene protons 7-H<sub>2</sub> ( $\delta$  3.10 and 3.30) were also coupled to C-3a. 3a-H was coupled to two methylene carbons (C-3,  $\delta$  43.8 and C-7), two olefinic carbons (C-4 and C-5) and a primary carbonyl carbon (C-9). 3-H<sub>i</sub> at  $\delta$  3.19, one of the nonequivalent methylene protons, was coupled to two bridge-head carbons (C-3a and C-7a) and a quaternary carbon (C-1,  $\delta$  67.3), whereas 3-H<sub>h</sub> at  $\delta$  1.77 was coupled to an oxygen-bearing methine carbon (C-2,  $\delta$  75.1), a bridge-head carbon C-3a and a non-protonated olefinic carbon C-4. These connectivities revealed that C-3a was adjacent to C-7a. Thus, two carbon chains shown by the  $^1\text{H}$ - $^1\text{H}$  COSY were connected each other.



A proton (7-H<sub>i</sub>) at  $\delta$  3.30 showed connectivities to an *N*-methyl carbon, an olefin carbon (C-5) and a bridge-head carbon (C-7a). 7-H<sub>h</sub> at  $\delta$  3.10 was also coupled to C-7a. A bridge-head proton (7a-H) was coupled to an oxygen-bearing methine carbon (C-2) and a quaternary carbon (C-1). The last proton on the skeleton, H-2 at  $\delta$  4.50, showed coupling to an ester carbonyl carbon (C-8,  $\delta$  174.6). All connectivities discussed above indicated that **2** had a 6-azaindene carboxylic ester structure. In addition, a secondary amide proton resonating at  $\delta$  8.93 was coupled to a quaternary C-1, a oxygen-bearing methine carbon (C-2), an ester carbonyl C-8 and a secondary amide carbonyl C-10 at  $\delta$  164.2. Isolated methylene protons ( $\delta$  4.77 and 4.89) were coupled to a secondary amide carbonyl C-10. These observations showed that the substituted-acetamide group was attached at C-1. Methyl protons at  $\delta$  3.57 were coupled to ester carbonyl C-8. *N*-methyl protons at  $\delta$  2.54 were coupled to a protonated olefin carbon (C-5) and a methylene carbon (C-7) bearing a nitrogen. The primary amide protons (9-NH<sub>2</sub>,  $\delta$  7.11) were coupled to C-4. All resonances in the NMR spectra, except for one NH<sub>2</sub> and one OH groups, were now assigned. The remaining parts of **2** are -OH, -NH<sub>2</sub> and -SO<sub>2</sub>-. All assignments of  $^{13}\text{C}$  and  $^1\text{H}$  chemical shifts and the long range connectivity between proton and carbon are summarized in Table 3.

Table 3.  $^{13}\text{C}$  and  $^1\text{H}$  Chemical shift assignments (ppm) for altemicidin methyl ester (**2**) and protons to which a long range connectivity is observed in the HMBC experiment in pyridine- $d_5$

Assignment	$^{13}\text{C}$	$^1\text{H}$	Long range connectivity in HMBC ( $^1\text{H}$ )
1	67.3		3- $\text{H}_l$ , 7a-H, 1-NH
2	75.1	4.50	3- $\text{H}_h$ , 7a-H, 1-NH
3	43.8	1.77, 3.19	3a-H
3a	32.7	3.64	3- $\text{H}_h$ , 3- $\text{H}_l$ , 5-H, 7- $\text{H}_h$ , 7- $\text{H}_l$
4	102.2		3- $\text{H}_h$ , 3a-H, 5-H, 9- $\text{NH}_2$
5	143.7	7.64	3a-H, 7- $\text{H}_l$ , 12- $\text{H}_3$
7	45.4	3.10, 3.30	3a-H, 5-H, 12- $\text{H}_3$
7a	41.1	3.59	3- $\text{H}_l$ , 3a-H, 7- $\text{H}_h$ , 7- $\text{H}_l$
8	174.6		2-H, 1-NH, ester- $\text{H}_3$
9	171.0		3a-H, 5-H
10	164.2		11- $\text{H}_2$ , 1-NH
11	60.9	4.77, 4.89	
12	42.2	2.54	5-H, 7- $\text{H}_l$
1-NH		8.93	
2-OH		8.58	
9- $\text{NH}_2$		7.11	
11- $\text{SO}_2\text{NH}_2$		8.72	
ester- $\text{CH}_3$	52.4	3.57	

The hydroxyl group was unequivocally connected to C-2. The isolated methylene group was assigned to the substituted acetyl group by NMR studies mentioned above. According to the fact that protons of the corresponding methylene group of **1** were readily convertible to deuteriums in  $\text{D}_2\text{O}$  during the measurement of the NMR spectrum, this methylene group was directly attached to the strongly electron-withdrawing substituent. Thus, we decided that the  $-\text{SO}_2\text{NH}_2$  (sulfamoyl) group was connected to the C-11 methylene group.

From all spectroscopic experiments already described, we proposed the relative structure of **2** to be methyl 4-carbamoyl-2-hydroxy-6-methyl-1-[(2-sulfamoylacetyl)amino]-2,3,3a,6,7,7a-hexahydro-6-azaindene-1-carboxylate.

Compound **2** was treated with 9-hydroxyxanthene, which is a reagent for the detection of a primary amide group or a sulfamoyl group, in acetic acid to give greenish crystals of the 9-*N*-(9-xanthenyl) derivative (**3**), SIMS  $m/z$  571 [(M+H) $^+$ ]. The structure of **1** including its absolute configuration was determined by X-ray crystallographic analysis of **3** to be (1*R*,2*S*,3*aR*,7*aS*)-4-carbamoyl-2-hydroxy-6-methyl-1-[(2-sulfamoylacetyl)amino]-2,3,3a,6,7,7a-hexahydro-6-azaindene-1-carboxylic acid.<sup>8)</sup> 9-Hydroxyxanthene reacted with the carbamoyl group of **3** rather than the sulfamoyl group.

## EXPERIMENTAL

Altemicidin (**1**), altemicidin methyl ester (**2**) and xanthenylaltemicidin methyl ester (**3**) were prepared by us.<sup>8)</sup>

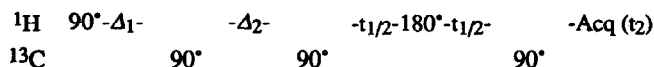
**Mass spectrometry.** The secondary ion mass spectrum (SIMS) was obtained on a Hitachi M-80H double focusing mass spectrometer using glycerol and Xe gas. The resolution power was 1500 in this experiment. The obtained spectrum indicated an  $(M+H)^+$  ion peak at  $m/z$  377.

The high resolution fast atom bombardment mass spectrum (HRFABMS) was obtained on a Jeol JMS-HX110 mass spectrometer under the following conditions: Ion accelerative voltage -10KV, resolution power 3,000, Xe gas and glycerol matrix. The exact mass number was determined by the use of  $m/z$  369.2125 and 413.2389 of polyethyleneglycol 400 as a reference substance. The observed negative ion peak at  $m/z$  375.1009  $[(M-H)^-]$  supported the molecular formula,  $C_{13}H_{19}N_4O_7S$ ; 375.0975.

**NMR spectroscopy.** NMR spectra were recorded on a Jeol JNM-GX400 spectrometer equipped with 5 mm ( $\phi$ )  $^1H/^{13}C$  dual probe head. All NMR experiments were recorded on samples containing 20 mg of **1** in 0.55 ml of  $D_2O$  and 5 mg of **2** in 0.55 ml of pyridine- $d_5$ .

**$^1H$ - $^1H$  double quantum filtered COSY of **2**.** The DQF COSY spectrum of **2** was obtained from a 512 x 1024 data matrix size after zero filling in the  $F_1$  dimension. The spectral width was 3230.0 Hz in both dimensions and acquisition time was 159 ms. The carrier was positioned at 4.9 ppm. Sixteen scans were recorded for each  $t_1$  value with a delay time of 1 s between scans. In both dimensions unshifted sine-bell filtering was used prior to Fourier transformation. The total measuring time was 1.5 h.

**HMBC spectrum of **2**.** The spectrum of Fig. 6 resulted from a 512 x 1024 data matrix after zero filling in  $F_1$  dimension. The spectral widths were 3230.0 Hz in  $F_2$  and 20 KHz in  $F_1$ . The pulse sequence was as follows:



A delay time of 1.16 s (including a 159 ms  $t_2$  acquisition period) and 176 scans per  $t_1$  value were used.  $\Delta_1$  and  $\Delta_2$  durations in the sequence were 3.70 and 60.0 ms, respectively. Exponential filterings were used in both dimensions: 0.5 Hz in  $F_2$  and 3 Hz in  $F_1$ . The RF carriers were positioned at 4.9 ppm in  $F_2$  and 99 ppm in  $F_1$ . The total measuring time was 14.5 h.

## REFERENCES

- (1) Takahashi, A.; Saito, N.; Hotta, K.; Okami, Y.; Umezawa, H. *J. Antibiotics* **1986**, *39*, 1033-1040.
- (2) Takahashi, A.; Ikeda, D.; Naganawa, H.; Okami, Y.; Umezawa, H. *J. Antibiotics* **1986**, *39*, 1041-1046.
- (3) Kameyama, T.; Takahashi, A.; Kurasawa, S.; Ishizuka, M.; Okami, Y.; Takeuchi, T.; Umezawa, H. *J. Antibiotics* **1987**, *40*, 1664-1670.
- (4) Takahashi, A.; Nakamura, H.; Kameyama, T.; Kurasawa, S.; Naganawa, H.; Okami, Y.; Takeuchi, T.; Umezawa, H.; Iitaka, Y. *J. Antibiotics* **1987**, *40*, 1671-1676.
- (5) Kameyama, T.; Takahashi, A.; Matsumoto, H.; Kurasawa, S.; Hamada, M.; Okami, Y.; Ishizuka, M.; Takeuchi, T. *J. Antibiotics* **1988**, *41*, 1561-1567.
- (6) Takahashi, A.; Nakamura, H.; Ikeda, D.; Naganawa, H.; Kameyama, T.; Kurasawa, S.; Okami, Y.; Takeuchi, T.; Iitaka, Y. *J. Antibiotics* **1988**, *41*, 1568-1574.
- (7) Takahashi, A.; Kurasawa, S.; Ikeda, D.; Okami, Y.; Takeuchi, T. *J. Antibiotics* **1989**, *42*, 1556-1561.
- (8) Takahashi, A.; Ikeda, D.; Nakamura, H.; Naganawa, H.; Kurasawa, S.; Okami, Y.; Takeuchi, T.; Iitaka, Y. *J. Antibiotics* **1989**, *42*, 1562-1566.
- (9) Doddrell, D. M.; Pegg, D. T.; Bendall, M. R. *J. Magn. Reson.* **1982**, *48*, 323-327.
- (10) Piantini, U.; Sørensen, O. W.; Ernst, R. R. *J. Am. Chem. Soc.* **1982**, *104*, 6800-6801.
- (11) Summers, M. F.; Marzilli, L. G.; Bax, A. *J. Am. Chem. Soc.* **1986**, *108*, 4285-4294 and references cited therein.
- (12) Bax, A.; Summers, M. F. *J. Am. Chem. Soc.* **1986**, *108*, 2093-2094.